Preprints of the 21st IFAC World Congress (Virtual)
Berlin, Germany, July 12-17, 2020

Robust Global Tracking Control for a Quadrotor Based on Uncertainty and Disturbance Estimator

Qi Lu *

* *Department of Mechanical Engineering, Sichuan University-Pittsburgh Institute, Sichuan University, Chengdu, Sichuan, 610207 China (e-mail: qi.lu@scu.edu.cn).*

Abstract: In this paper, an uncertainty and disturbance estimator (UDE)-based robust global tracking control strategy for a quadrotor is presented. Utilizing the quaternion framework, the attitude and position controllers are developed to achieve the global singularity-free and computational efficient quadrotor control while the UDE is adopted to deal with model uncertainties and external disturbances. In order to handle the highly nonlinear quaternion-based quadrotor dynamics, the backstepping technique is utilized for the attitude controller derivation. The thrust-vectoring approach is employed for the position controller derivation. The effectiveness of the proposed approach is demonstrated using the attitude recovery experiment with large angle initial conditions.

Keywords: Uncertainty and disturbance estimator (UDE), quadrotor, robust control, quaternion.

1. INTRODUCTION

The level of quadrotor's maneuverability is closely related to the flight control algorithms, whereas the controllers developed from linearization around hovering conditions have limited achievable flight envelopes. To achieve the agile flight of quadrotor, there are several challenges need to be handled. Firstly, the Euler angles exhibit kinematic singularities due to the fact that the attitude dynamics evolves on a nonlinear manifold, $SO(3)$ (Lee (2013)). Secondly, the quadrotor rigid body dynamics is naturally unstable, nonlinear with coupled states (Naldi et al. (2017)). Thirdly, the incomprehensive modeling process of the quadrotor dynamics leads to model uncertainties. The fourth challenge comes from the external disturbances, such as wind. For practical applications, the control algorithm complexity is also restricted by the limited memory and processing power of the embedded processors.

Over the past years, various flight control algorithms have been investigated. Based on the commonly used attitude representation methods, which are Euler angle, rotation matrix and quaternion, the existing control algorithms can be roughly grouped into three categories. The controllers developed with the Euler angle attitude representation method have the merits of simple and easy implementation. Therefore, the fusion of the Euler angles with different control strategies are widely studied, such as the PID control (Moreno-Valenzuela et al. (2018)), the adaptive control (Zhao et al. (2015)) and the robust control algorithms which are derived with the sliding mode technique (Chen et al. (2016)), the active disturbance rejection control technique (Yang et al. (2018)), and the uncertainty and disturbance estimator (UDE) (Lu et al. (2017, 2018); Sanz et al. (2016)). However, the kinematic singularities prevent the Euler angle-based control strategies for achieving large angle maneuvers. To deal with the singularities, Goodarzi et al. (2015); Lee (2013); Shi et al. (2017); D.H.S. Maithripala and Jordan M. Berg (2015) derived the geometric controllers. Using the exponential coordinates, Shi et al. (2017) developed the geometric controllers. Nevertheless, the external disturbances and model uncertainties are not considered in the derivation process. D.H.S. Maithripala and Jordan M. Berg (2015) proposed an intrinsic PID controller to handle the bounded parametric uncertainties and disturbances by introducing the integral action. To handle the disturbance term, the adaptive geometric controller development is investigated in Lee (2013) and Goodarzi et al. (2015). However, the bound information of the disturbance term is needed in Lee (2013). With the same singularity free property, compared to the rotation matrix, the computational complexity of the quaternion is relatively less. Tayebi and McGilvray (2006) developed a PD^2 controller with quaternion to achieve the attitude stabilization. A nonlinear quaternion-based control algorithm for a variable pitch quadrotor is proposed in Cutler and How (2015). However, in real applications, the model uncertainties and external disturbances are inevitable. Liu et al. (2015) and Naldi et al. (2017) respectively proposed robust quaternion-based attitude controller and robust hybrid full degrees-of-freedom (DOFs) control strategy to deal with the model uncertainties and external disturbances. The experimental demonstration of large angle maneuvers using only onboard sensing and computation still remains as a challenging task (Liu et al. (2015)).

In this paper, in response to the singularities for Euler angles, and the computational complexities for matrix manipulations, the UDE-based full DOFs quadrotor controllers with the quaternion framework are developed. The performance of the developed control strategies is demonstrated through the implementation on a quadrotor to achieve large angle maneuvers with only onboard sensing and computation. The UDE-based control algorithm, which is proposed in Zhong and Rees (2004), has drawn considerable amount of attention in both theoretical (Ren et al. (2017); Dai et al. (2018)) and application (Lu et al. (2017, 2018); Sanz et al. (2016)) perspectives due to the advantages of simple structure and easy tuning. The main contributions of this paper include:

1) Using the quaternion attitude representation method, the UDE-based attitude controllers have been developed to achieve

the global non-singular attitude tracking while dealing with the effects of model uncertainties and external disturbances. The backstepping technique is applied to handle the nonlinear quaternion dynamics.

2) With the cascade control architecture and the thrust-vectoring approach, the UDE-based position controllers have been derived to solve the underactuation problem and to achieve the accurate position control.

3) The proposed approach is validated with quadrotor flight experiments using only onboard sensing and computation. The advantages of the developed quaternion-based controllers are demonstrated with attitude recovery from large undesirable initial angles. Compared with our previously published works (Lu et al. (2017, 2018)), which are developed based on Euler angle attitude representation, the capabilities and the operation ranges of the proposed controllers are further improved with the demonstration of more challenging flight maneuvers.

The rest of this paper is organized as follows. The quadrotor system modeling and the problem formulation are presented in Section 2. Section 3 introduces the UDE-based attitude and position controllers.The flight experimental results are shown in Section 4. The conclusions are drawn in Section 5.

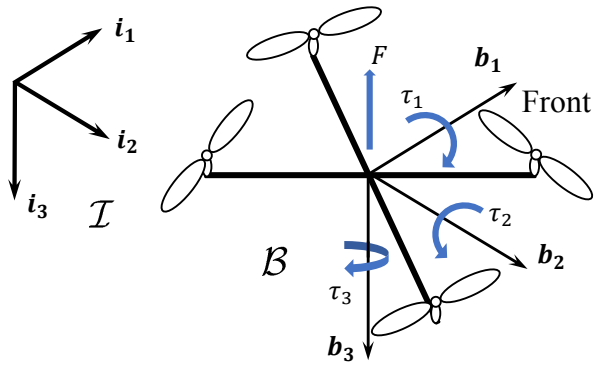

Fig. 1. Quadrotor coordinate systems.

2. SYSTEM MODELING AND PROBLEM FORMULATION

2.1 Quadrotor Mathematical Model

Fig. 1 shows the coordinate systems used for developing the quadrotor dynamic models. Let $\mathcal{I} = \{\, \boldsymbol{i_1}\ \boldsymbol{i_2}\ \boldsymbol{i_3} \,\}$ represent the right-hand inertia reference frame with $\boldsymbol{i_3}$ pointing downwards. The body-fixed frame is denoted by $\mathcal{B} = \{\, \boldsymbol{b_1}\ \boldsymbol{b_2}\ \boldsymbol{b_3} \,\}$ with the origin attached to the center of gravity of the quadrotor. The quadrotor attitude is represented using a unit quaternion, which is defined as $\mathbf{q} = [q_0\ q_1\ q_2\ q_3]^\intercal = [q_0\ \mathbf{q}_v]^\intercal \in \mathbf{S}^3$ where $^\intercal$ is the transpose operator, $\mathbf{S}^3 = \left\{\mathbf{q} \in \mathbb{R}^4 | \mathbf{q}^\intercal\mathbf{q} = 1\right\}$ denotes the three-dimensional unit sphere space, q_0 and $\mathbf{q}_v = [q_1\ q_2\ q_3]^\intercal$ represent the scalar and vector parts of the quaternion, respectively. The angular velocities are defined by $\boldsymbol{\omega} = [\omega_1\ \omega_2\ \omega_3]^\intercal \in \mathbb{R}^3$. Let $\boldsymbol{\xi} = [\xi_1\ \xi_2\ \xi_3]^\intercal \in \mathbb{R}^3$ and $\mathbf{v} = [v_1\ v_2\ v_3]^\intercal \in \mathbb{R}^3$ represent the positions and velocities of the quadrotor, respectively. The collective thrust along the negative $\boldsymbol{b_3}$ direction is denoted by F and the torques along the three body axes are defined as τ_1, τ_2 and τ_3. Considering a quadrotor with the mass of m and the inertia matrix of $\mathbf{J} \in \mathbb{R}^{3\times3}$, the dynamics can be modeled with quaternion formulation as (Naldi et al. (2017); Cutler and How (2015))

$$\dot{\boldsymbol{\xi}} = \mathbf{v} \tag{1}$$

$$\begin{bmatrix}0\\ \dot{\mathbf{v}}\end{bmatrix} = -\frac{1}{m}\mathbf{q} \otimes \begin{bmatrix}0\\ \mathbf{F}\end{bmatrix} \otimes \mathbf{q}^* + \begin{bmatrix}0\\ \mathbf{g}\end{bmatrix} + \frac{1}{m}\begin{bmatrix}0\\ \mathbf{d}_\xi\end{bmatrix} \tag{2}$$

$$\dot{\mathbf{q}} = \frac{1}{2}\mathbf{q} \otimes \begin{bmatrix}0\\ \boldsymbol{\omega}\end{bmatrix} = \frac{1}{2}\begin{bmatrix}-\mathbf{q}_v^\intercal\boldsymbol{\omega}\\ q_0\boldsymbol{\omega} + \mathbf{q}_v \times \boldsymbol{\omega}\end{bmatrix} \tag{3}$$

$$\dot{\boldsymbol{\omega}} = -\mathbf{J}^{-1}\left(\boldsymbol{\omega} \times \mathbf{J}\boldsymbol{\omega}\right) + \mathbf{J}^{-1}\left(\boldsymbol{\tau} + \mathbf{d}_q\right) \tag{4}$$

where $\otimes$ is the quaternion multiplication, $\times$ is the cross product, $\mathbf{F} = [0\ 0\ F]^\intercal \in \mathbb{R}^3$ represents the thrust force vector in $\mathcal{B}$, $\mathbf{g} = [0\ 0\ g]^\intercal \in \mathbb{R}^3$ is the gravity vector in $\mathcal{I}$, $\boldsymbol{\tau} = [\tau_1\ \tau_2\ \tau_3]^\intercal \in \mathbb{R}^3$ is the torque vector, $\mathbf{d}_\xi \in \mathbb{R}^3$ and $\mathbf{d}_q \in \mathbb{R}^3$ are the bounded external disturbances acting on the position and attitude subsystems, respectively.

2.2 Problem Formulation

The control problems are two folded in this work. The first objective is to develop the UDE-based global attitude control algorithms to regulate the quadrotor orientation $\mathbf{q}(t)$ to track the orientation reference $\mathbf{q}_r(t) = [q_{r0}(t)\ q_{r1}(t)\ q_{r2}(t)\ q_{r3}(t)]^\intercal \in \mathbf{S}^3$ for all possible initial conditions $\mathbf{q}(0)$. The second goal is developing the UDE-based position control algorithm to drive the quadrotor position $\boldsymbol{\xi}(t)$ to track the position reference $\boldsymbol{\xi}_r(t) = [\xi_{r1}(t)\ \xi_{r2}(t)\ \xi_{r3}(t)]^\intercal \in \mathbb{R}^3$. The reference trajectories, $\mathbf{q}_r(t)$ and $\boldsymbol{\xi}_r(t)$ are bounded and continuously differentiable up to their second order time derivatives for all $t \geq 0$.

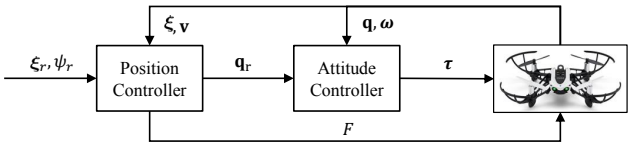

Fig. 2. Cascade control scheme for a quadrotor.

3. CONTROL DESIGN

In this section, the detailed derivations of the UDE-based attitude and position control algorithms are presented. The overall control scheme is shown in Fig. 2, where ψ_r is the yaw angle reference.

3.1 Quaternion-Based Attitude Controller Design

The tracking errors for attitude subsystems are defined as

$$\mathbf{q}_e = \mathbf{q}_r^* \otimes \mathbf{q} = \begin{bmatrix}q_{e0}\\ \mathbf{q}_{ev}\end{bmatrix} \tag{5}$$

$$\boldsymbol{\omega}_e = \boldsymbol{\omega}_r - \boldsymbol{\omega} \tag{6}$$

where $\boldsymbol{\omega}_r$ denotes the reference angular velocity vector, q_{e0} and $\mathbf{q}_{ev}$ are the scalar and vector parts of $\mathbf{q}_e$, respectively. The relationship between the desired attitude and the desired angular velocities is described with the following differential equation $\dot{\mathbf{q}}_r = \frac{1}{2}\mathbf{q}_r \otimes [0\ \boldsymbol{\omega}_r]^\intercal$. Taking the time derivative of (5) results in (Tayebi (2008))

$$\dot{\mathbf{q}}_e = -\frac{1}{2}\begin{bmatrix}0\\ \boldsymbol{\omega}_r\end{bmatrix} \otimes \mathbf{q}_e + \frac{1}{2}\mathbf{q}_e \otimes \begin{bmatrix}0\\ \boldsymbol{\omega}\end{bmatrix} = \frac{1}{2}\begin{bmatrix}-\mathbf{q}_{ev}^{\intercal}\left(\boldsymbol{\omega}-\boldsymbol{\omega}_r\right)\\ q_{e0}\left(\boldsymbol{\omega}-\boldsymbol{\omega}_r\right)+\mathbf{q}_{ev}\times\left(\boldsymbol{\omega}+\boldsymbol{\omega}_r\right)\end{bmatrix} \tag{7}$$

The objective is to design the effective attitude controllers which are capable of driving the quaternion attitude tracking errors $\mathbf{q}_e$ to $[\pm 1\ 0\ 0\ 0]^{\top}$ and the angular velocity tracking errors $\boldsymbol{\omega}_e$ to zero. It should be noted that the two equilibrium points $\mathbf{q}_e = [\pm 1\ 0\ 0\ 0]^{\top}$ are in reality one physical equilibrium point (Tayebi and McGilvray (2006)). With the unit property of $\mathbf{q}_e$, as $\mathbf{q}_{ev}$ converging to zero, q_{e0} will be ± 1. From (4), (6) and (7), the tracking error dynamics for attitude subsystems can be written in the form of

$$\dot{\mathbf{q}}_{ev} = -\frac{1}{2}q_{e0}\boldsymbol{\omega}_e + \frac{1}{2}\mathbf{q}_{ev}\times\left(\boldsymbol{\omega}+\boldsymbol{\omega}_r\right) \tag{8}$$

$$\dot{\boldsymbol{\omega}}_e = \dot{\boldsymbol{\omega}}_r + \mathbf{J}^{-1}\left(\boldsymbol{\omega}\times\mathbf{J}\boldsymbol{\omega}\right) - \mathbf{J}^{-1}\left(\boldsymbol{\tau}+\mathbf{d}_q\right) \tag{9}$$

To deal with the structure constraint in the UDE-based controllers, the backstepping technique is adopted. The virtual control for (8) is designed as (Mahony et al. (2008))

$$\boldsymbol{\alpha} = 2\mathbf{C}_1 q_{e0}\mathbf{q}_{ev} \tag{10}$$

where $\mathbf{C}_1 \in \mathbb{R}^{3\times 3}$ is a constant matrix. Then the coordinate transformation is introduced as

$$\begin{aligned}\mathbf{z}_1 &= \mathbf{q}_{ev}\\ \mathbf{z}_2 &= -\boldsymbol{\omega}_e + \boldsymbol{\alpha}\end{aligned} \tag{11}$$

Taking the time derivative of (11) results in

$$\begin{aligned}\dot{\mathbf{z}}_1 &= -\frac{1}{2}q_{e0}\boldsymbol{\omega}_e + \frac{1}{2}\mathbf{z}_1\times\left(\boldsymbol{\omega}+\boldsymbol{\omega}_r\right) + \frac{1}{2}q_{e0}\boldsymbol{\alpha} - \frac{1}{2}q_{e0}\boldsymbol{\alpha}\\ &= -q_{e0}^2\mathbf{C}_1\mathbf{z}_1 + \frac{1}{2}q_{e0}\mathbf{z}_2 + \frac{1}{2}\mathbf{z}_1\times\left(\boldsymbol{\omega}+\boldsymbol{\omega}_r\right)\end{aligned} \tag{12}$$

$$\begin{aligned}\dot{\mathbf{z}}_2 &= -\dot{\boldsymbol{\omega}}_e + \dot{\boldsymbol{\alpha}}\\ &= -\dot{\boldsymbol{\omega}}_r - \mathbf{J}^{-1}\left(\boldsymbol{\omega}\times\mathbf{J}\boldsymbol{\omega}\right) + \mathbf{J}^{-1}\left(\boldsymbol{\tau}+\mathbf{d}_q\right) + \dot{\boldsymbol{\alpha}}\end{aligned} \tag{13}$$

The Lyapunov function candidate is chosen as

$$V_q = \frac{1}{2}\mathbf{z}_1^{\intercal}\mathbf{z}_1 + \frac{1}{2}\mathbf{z}_2^{\intercal}\mathbf{z}_2 \tag{14}$$

Taking the time derivative of (14) results in

$$\begin{aligned}\dot{V}_q &= \mathbf{z}_1^{\intercal}\dot{\mathbf{z}}_1 + \mathbf{z}_2^{\intercal}\dot{\mathbf{z}}_2\\ &= \mathbf{z}_1^{\intercal}\left[-q_{e0}^2\mathbf{C}_1\mathbf{z}_1 + \frac{1}{2}q_{e0}\mathbf{z}_2 + \frac{1}{2}\mathbf{z}_1\times\left(\boldsymbol{\omega}+\boldsymbol{\omega}_r\right)\right] + \mathbf{z}_2^{\intercal}\dot{\mathbf{z}}_2\\ &= -\mathbf{z}_1^{\intercal}q_{e0}^2\mathbf{C}_1\mathbf{z}_1 + \frac{1}{2}\mathbf{z}_1^{\intercal}\mathbf{z}_1\times\left(\boldsymbol{\omega}+\boldsymbol{\omega}_r\right) + \mathbf{z}_2^{\intercal}\left(\frac{1}{2}q_{e0}\mathbf{z}_1 + \dot{\mathbf{z}}_2\right)\end{aligned} \tag{15}$$

Expanding the cross product term $\frac{1}{2}\mathbf{z}_1^{\intercal}\mathbf{z}_1\times\left(\boldsymbol{\omega}+\boldsymbol{\omega}_r\right)$ leads to zero. In order to ensure (15) is negative, the desired error dynamics is designed as

$$\frac{1}{2}q_{e0}\mathbf{z}_1 + \dot{\mathbf{z}}_2 = -\mathbf{C}_2\mathbf{z}_2 \tag{16}$$

where $\mathbf{C}_2 \in \mathbb{R}^{3\times 3}$ is a positive gain matrix. Combine (13) and (16) and design the control action term as

$$\mathbf{J}^{-1}\boldsymbol{\tau} = -\mathbf{C}_2\mathbf{z}_2 - \frac{1}{2}q_{e0}\mathbf{z}_1 + \dot{\boldsymbol{\omega}}_r + \mathbf{J}^{-1}\left(\boldsymbol{\omega}\times\mathbf{J}\boldsymbol{\omega}\right) - \mathbf{u}_d \tag{17}$$

where $\mathbf{u}_d = \mathbf{J}^{-1}\mathbf{d}_q + \dot{\boldsymbol{\alpha}}$ represents the lumped uncertainty term, which can be solved from (13) as

$$\mathbf{u}_d = \dot{\mathbf{z}}_2 + \dot{\boldsymbol{\omega}}_r + \mathbf{J}^{-1}\left(\boldsymbol{\omega}\times\mathbf{J}\boldsymbol{\omega}\right) - \mathbf{J}^{-1}\boldsymbol{\tau} \tag{18}$$

Following the UDE techniques described in Zhong and Rees (2004), the lumped uncertainty term estimation is constructed by adopting strictly low-pass filters with unity steady-state gains as

$$\hat{\mathbf{u}}_d = \mathcal{L}^{-1}\left\{\mathbf{G}_{fq}\left(s\right)\right\} * \left\{\dot{\mathbf{z}}_2 + \dot{\boldsymbol{\omega}}_r + \mathbf{J}^{-1}\left(\boldsymbol{\omega}\times\mathbf{J}\boldsymbol{\omega}\right) - \mathbf{J}^{-1}\boldsymbol{\tau}\right\} \tag{19}$$

where $\mathcal{L}^{-1}$ denotes the inverse Laplace operator, $*$ represents the convolution operator, $\hat{\mathbf{u}}_d$ is the estimation of lumped uncertainty term $\mathbf{u}_d$, $\mathbf{G}_{fq}\left(s\right) \in \mathbb{R}^{3\times 3}$ is a 3 by 3 filter matrix in the form of $\mathbf{G}_{fq}\left(s\right) = \mathrm{diag}\left(G_{fq1}\left(s\right),\ G_{fq2}\left(s\right),\ G_{fq3}\left(s\right)\right)$ and $\mathrm{diag}(\cdot)$ represents the diagonal matrix operator. Substituting (19) into (17) and solving for $\boldsymbol{\tau}$, the UDE-based attitude control laws are derived as

$$\begin{aligned}\boldsymbol{\tau} = {} & \boldsymbol{\omega}\times\mathbf{J}\boldsymbol{\omega} + \mathbf{J}\dot{\boldsymbol{\omega}}_r\\ & -\mathbf{J}\mathcal{L}^{-1}\left\{\left(\mathbb{I}_3 - \mathbf{G}_{fq}\left(s\right)\right)^{-1}\right\} * \left[\mathbf{C}_2\mathbf{z}_2 + \frac{1}{2}q_{e0}\mathbf{z}_1\right]\\ & -\mathbf{J}\mathcal{L}^{-1}\left\{\left(\mathbb{I}_3 - \mathbf{G}_{fq}\left(s\right)\right)^{-1}\mathbf{G}_{fq}\left(s\right)s\right\} * \mathbf{z}_2\end{aligned} \tag{20}$$

3.2 Position Controller Design

The tracking errors for the quadrotor position subsystems are defined as

$$\begin{aligned}\boldsymbol{\xi}_e &= \boldsymbol{\xi}_r - \boldsymbol{\xi}\\ \mathbf{v}_e &= \mathbf{v}_r - \mathbf{v}\end{aligned} \tag{21}$$

Define $\mathbf{e}_{\xi} = [\boldsymbol{\xi}_e\ \mathbf{v}_e]^{\intercal}$ as the error vector for the position subsystems. Hence, the objective is designing the effective position controllers to drive $\mathbf{e}_{\xi}$ to zero. Let $\mathbf{F}_{\xi}$ represent the thrust forces vector in $\mathcal{I}$, where $\begin{bmatrix}0\\ \mathbf{F}_{\xi}\end{bmatrix} = \mathbf{q}\otimes\begin{bmatrix}0\\ \mathbf{F}\end{bmatrix}\otimes\mathbf{q}^*$. Using the vector representation, the position dynamics (2) can be rewritten as

$$\dot{\mathbf{v}} = -\frac{1}{m}\mathbf{F}_{\xi} + \mathbf{g} + \frac{1}{m}\mathbf{d}_{\xi} \tag{22}$$

The virtual control inputs are designed as

$$\mathbf{u}_{\xi} = -\frac{1}{m}\mathbf{F}_{\xi} + \mathbf{g} \tag{23}$$

Taking the time derivative of $\mathbf{e}_{\xi}$ along with (1), (21) and (22) leads to

$$\dot{\mathbf{e}}_{\xi} = \mathbf{h}_{\xi}\left(\mathbf{v}_e,\ \mathbf{v}_r\right) - \mathbf{B}_{\xi}\left(\mathbf{u}_{\xi} + \frac{1}{m}\mathbf{d}_{\xi}\right) \tag{24}$$

where $\mathbf{B}_{\xi} = [\mathbf{0}_{3\times 3}\ \mathbb{I}_3]^{\intercal} \in \mathbb{R}^{6\times 3}$, $\mathbf{h}_{\xi}\left(\mathbf{v}_e,\ \mathbf{v}_r\right) = [\mathbf{v}_e\ \dot{\mathbf{v}}_r]^{\intercal} \in \mathbb{R}^{6\times 3}$, $\mathbf{0}_{m\times n} \in \mathbb{R}^{m\times n}$ represents the m by n zero matrix, and

$\mathbb{I}_n \in \mathbb{R}^{n\times n}$ is the n-dimensional identity matrix. Specify the desired error dynamics as

$$\dot{\mathbf{e}}_\xi = -\mathbf{K}_\xi \mathbf{e}_\xi \tag{25}$$

where $\mathbf{K}_\xi \in \mathbb{R}^{6\times 6}$ denotes the error feedback gain matrix. Combining (24) and (25) results in

$$\mathbf{h}_\xi\left(\mathbf{v}_e,\ \mathbf{v}_r\right) - \mathbf{B}_\xi\left(\mathbf{u}_\xi + \frac{1}{m}\mathbf{d}_\xi\right) = -\mathbf{K}_\xi \mathbf{e}_\xi \tag{26}$$

Hence, according to (26), design the control action term as

$$\mathbf{B}_\xi \mathbf{u}_\xi = \mathbf{h}_\xi\left(\mathbf{v}_e,\ \mathbf{v}_r\right) + \mathbf{K}_\xi \mathbf{e}_\xi - \frac{1}{m}\mathbf{B}_\xi \mathbf{d}_\xi \tag{27}$$

The disturbance term can be solved from the position tracking error dynamics (24) as

$$\frac{1}{m}\mathbf{B}_\xi \mathbf{d}_\xi = \mathbf{h}_\xi\left(\mathbf{v}_e,\ \mathbf{v}_r\right) - \mathbf{B}_\xi \mathbf{u}_\xi - \dot{\mathbf{e}}_\xi$$

Following the UDE techniques in Zhong and Rees (2004), the disturbance term can be estimated as

$$\frac{1}{m}\mathbf{B}_\xi \hat{\mathbf{d}}_\xi = \mathcal{L}^{-1}\left\{\mathbf{G}_{f\xi}\left(s\right)\right\} * \left[\mathbf{h}_\xi - \mathbf{B}_\xi \mathbf{u}_\xi - \dot{\mathbf{e}}_\xi\right] \tag{28}$$

where

$$\mathbf{G}_{f\xi}\left(s\right) = \begin{bmatrix} \mathbf{0_{3\times 3}} & \mathbf{0_{3\times 3}} \\ \mathbf{0_{3\times 3}} & \left[G_{f\xi 1}\left(s\right)\ G_{f\xi 2}\left(s\right)\ G_{f\xi 3}\left(s\right)\right]\mathbb{I}_3 \end{bmatrix}$$

Replacing the disturbance term in (27) with (28) and solving for $\mathbf{u}_\xi$ leads to the UDE-based position control algorithms

$$\begin{aligned}\mathbf{u}_\xi = \mathbf{B}_\xi^+ \Big\{ & \mathcal{L}^{-1}\left\{\left(\mathbb{I}_6 - \mathbf{G}_{f\xi}\left(s\right)\right)^{-1}\right\} * \left(\mathbf{K}_\xi \mathbf{e}_\xi\right) + \mathbf{h}_\xi \\ & + \mathcal{L}^{-1}\left\{\left(\mathbb{I}_6 - \mathbf{G}_{f\xi}\left(s\right)\right)^{-1}\mathbf{G}_{f\xi}\left(s\right)s\right\} * \mathbf{e}_\xi \Big\}\end{aligned} \tag{29}$$

where $\mathbf{B}_\xi^+ = \left(\mathbf{B}_\xi^\intercal \mathbf{B}_\xi\right)^{-1}\mathbf{B}_\xi^\intercal$ represents the pseudo-inverse of $\mathbf{B}_\xi$.

Remark 1. It should be noted that for the implementation of the UDE-based position controller, (29) is used, where the measurement regarding the state derivative of the error vector, $\dot{\mathbf{e}}_\xi$, is avoided. For attitude controller implementation, (20) is used.

The commanded control forces in $\mathcal{I}$ can be solved from (23) as $\mathbf{F}_\xi = m\left(\mathbf{g} - \mathbf{u}_\xi\right)$. The thrust command can be calculated by taking the Euclidean norm of the commanded control forces as $F = \|\mathbf{F}_\xi\|$. Let the direction vector $\mathbf{r}_F$ denote the direction of commanded forces in $\mathcal{I}$, which is calculated as $\mathbf{r}_F = \frac{-\mathbf{F}_\xi}{\|\mathbf{F}_\xi\|}$. Due to the fact that the thrust direction is fixed in $\mathcal{B}$, which is the $-\boldsymbol{b_3}$ axis, the vector transformation from $\mathcal{B}$ to $\mathcal{I}$ is represented as $\begin{bmatrix}0\\ \mathbf{r}_F\end{bmatrix} = \mathbf{q}_r^{b_1b_2} \otimes \begin{bmatrix}0\\ -\boldsymbol{b_3}\end{bmatrix} \otimes \left(\mathbf{q}_r^{b_1b_2}\right)^*$, where $\mathbf{q}_r^{b_1b_2}$ is the desired quadrotor orientation excluding the rotation about the $\boldsymbol{b_3}$ axis. The unit quaternion $\mathbf{q}_r^{b_1b_2}$ which rotates $-\boldsymbol{b_3}$ into $\mathbf{r}_F$ can be solved as (Markley (2002); Cutler and How (2015))

$$\mathbf{q}_r^{b_1b_2} = \frac{1}{\sqrt{2\left[1 + \left(-\boldsymbol{b_3}\right)^\intercal \mathbf{r}_F\right]}}\begin{bmatrix}1 + \left(-\boldsymbol{b_3}\right)^\intercal \mathbf{r}_F \\ \left(-\boldsymbol{b_3}\right) \times \mathbf{r}_F\end{bmatrix} \tag{30}$$

Since the rotation about the $\boldsymbol{b_3}$ axis is not crucial regarding the thrust pointing direction, the desired rotations about $\boldsymbol{b_1}$ and $\boldsymbol{b_2}$ axes are firstly considered. Let ψ_r denote the desired heading angle, the desired orientation is fully specified as

$$\mathbf{q}_r = \mathbf{q}_r^{b_1b_2} \otimes \left[\cos\left(\frac{\psi_r}{2}\right)\ 0\ 0\ \sin\left(\frac{\psi_r}{2}\right)\right]^\intercal$$

Fig. 3. Experimental platform

4. EXPERIMENTS

4.1 Experimental Platform

Fig. 3 shows the experimental platform, which is a Parrot Mambo quadrotor [1] . The onboard three-axis accelerometer and three-axis gyroscope are used for orientation estimation. The position localization is achieved with an ultrasonic sensor, an air pressure sensor and a downward-facing camera. The update rate for the control loop is 200 Hz.

Table 1. Controller Parameters

	T_{qi}	c_{1i}	c_{2i}	$T_{\xi i}$	k_{1i}	k_{2i}	a_{m1i}	a_{m2i}
1	1/60	1	2	1/40	1	2	100	20
2	1/50	1	2	1/40	1	2	100	20
3	1/20	1	2	1/20	1	2	25	10

4.2 Filter and Controller Parameter Selection

The filter matrices in (20) and (29) are chosen as (Zhong and Rees (2004))

$$\mathbf{G}_{fq}\left(s\right) = \mathrm{diag}\left(\frac{1}{T_{q1}s+1},\ \frac{1}{T_{q2}s+1},\ \frac{1}{T_{q3}s+1}\right)$$

$$\mathbf{G}_{f\xi}\left(s\right) = \begin{bmatrix}\mathbf{0_{3\times 3}} & \mathbf{0_{3\times 3}} \\ \mathbf{0_{3\times 3}} & \mathrm{diag}\left(\frac{1}{T_{\xi 1}s+1},\ \frac{1}{T_{\xi 2}s+1},\ \frac{1}{T_{\xi 3}s+1}\right)\end{bmatrix}$$

with general first order filters for practical implementation. Choose $\mathbf{C}_1$ and $\mathbf{C}_2$ in (20) as following diagonal matrices

$$\mathbf{C}_1 = \mathrm{diag}\left(c_{11},\ c_{12},\ c_{13}\right),\ \mathbf{C}_2 = \mathrm{diag}\left(c_{21},\ c_{22},\ c_{23}\right)$$

The matrix $\mathbf{K}_\xi$ in (29) are designed as $\begin{bmatrix}\mathbf{0}_{3\times 3} & \mathbb{I}_3 \\ \mathbf{K}_1 & \mathbf{K}_2\end{bmatrix}$ with $\mathbf{K}_1 \in \mathbb{R}^{3\times 3}$ and $\mathbf{K}_2 \in \mathbb{R}^{3\times 3}$ being the diagonal matrices in the forms of

$$\mathbf{K}_1 = \mathrm{diag}\left(k_{11},\ k_{12},\ k_{13}\right),\ \mathbf{K}_2 = \mathrm{diag}\left(k_{21},\ k_{22},\ k_{23}\right)$$

The control parameter selections are listed in Table 1.

4.3 Results and Discussion

The attitude recovery flight experiment is carried out to validate the effectiveness of the developed UDE-based robust global control strategies. The objective of this experiment is to achieve the attitude recovery and position hover with the random initial conditions generated by hand tossing. The test is performed

[1] https://www.mathworks.com/hardware-support/parrot-minidrones

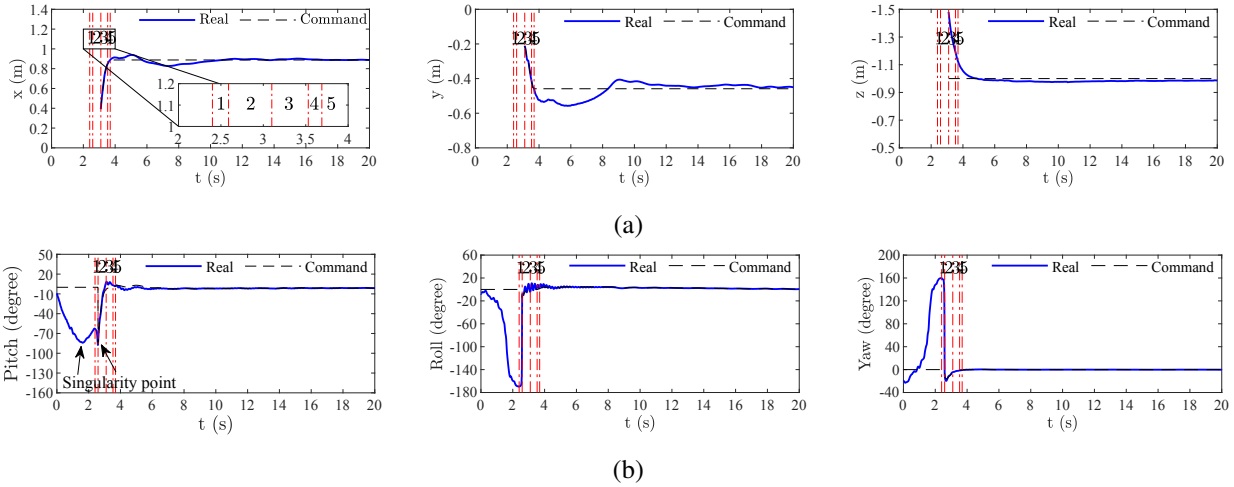

Fig. 4. Experimental results: (a) positions, (b) Euler angles, with five stages: 1: launch detection, 2: attitude control enabled, 3: height control enabled, 4: horizontal velocity control enabled, 5: full DOF control enabled.

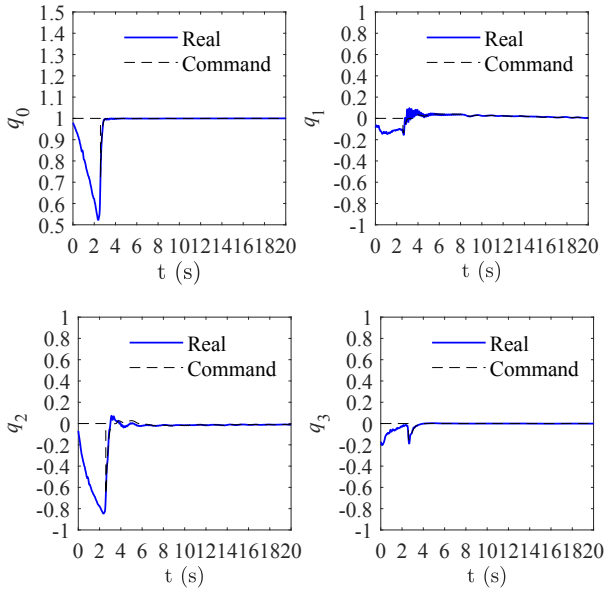

Fig. 5. Quadrotor attitude in quaternion.

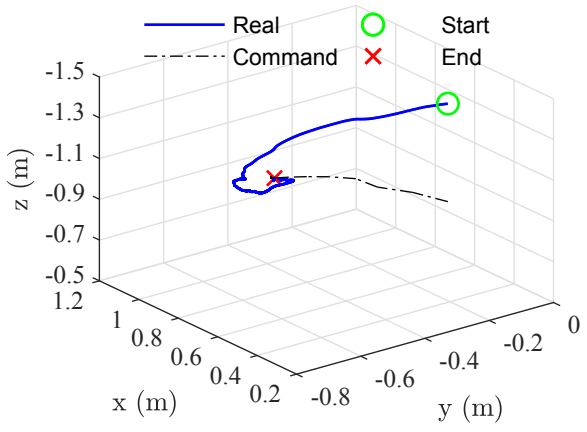

Fig. 6. Quadrotor trajectory in 3D view.

by throwing the quadrotor by hand in an indoor environment, then the launch detection, attitude recovery and position hover are achieved autonomously. Only onboard sensing and computation are used during this experiment. The similar recovery processes which are described in Faessler et al. (2015) are adopted. After the quadrotor is tossed by hand, the first stage is the launch detection. The quadrotor free falling will render the norm of the accelerometer data approaching zero. Once the average of the norm of the accelerometer data within last 20 ms is less than the threshold of 3 m/s^2, the attitude recovery process will be initiated, which is the second stage. The attitude controllers are enabled in the second stage. The quadrotor attitude references are set as $\mathbf{q}_r = [1\ 0\ 0\ 0]^\mathsf{T}$. The quadrotor thrust is set as $F = mg$ based on the nominal weight. After the roll and pitch angles are within the range of ± 10 degrees and the roll and pitch angular velocities are within the range of ± 1 rad/s, the third stage will start. In the third stage, the height controller is enabled with the reference set as -1 m. Since $\boldsymbol{i_3}$ axis is pointing downwards, the negative value in z direction actually means the quadrotor is above the ground. After the vertical velocity is less than 0.5 m/s, the fourth stage is enabled to reduce the horizontal velocities. The horizontal position controllers are activated with only velocity measurements feeding to the controllers while the horizontal velocity references are set as zero. As soon as the horizontal velocities are less than 0.2 m/s, the full DOF control of the quadrotor is enabled with the horizontal position references set as current positions.

The experimental results are shown in Fig. 4. The different stages are marked with numbers. For reader-friendly presentation, the positions are plotted as x, y, z and the orientations are shown as Euler angles. Since the onboard sensing is utilized, where the position measurements are conducted with respect to ground, only the position measurements after stage 2 are shown. Fig. 5 shows the evolution of the quaternion. The three-dimensional view of the quadrotor trajectories are shown in Fig. 6. The quadrotor is launched by hand at around $t = 2.4$ s, where the Euler angles are -159.556 degrees in roll direction, -62.748 degrees in pitch direction and -169.603 degrees in yaw direction. It should be noted the pitch angle has already passed the mathematical and mechanical singularity point, which is -90 degrees at $t = 1.62$ s as shown in Fig. 4 (b). In terms of rotation about the $\boldsymbol{b_2}$ axis, the angle is actually -117.252 degrees at

$t = 2.4$ s. From q_2 in Fig. 5, it can also be observed that the quadrotor is rotating in one direction before launched by hand. The length of the whole experiment is about 35 s. For a better view of the recovery processes, only the results from 0 s to 20 s are shown. The steady state root-mean-square errors from 15 s to 35 s when the quadrotor is stably hovering are calculated as 0.257 degree, 0.148 degree and 0.093 degree for roll, pitch and yaw directions, respectively and 0.005 m, 0.013 m, 0.013 m for x, y and z directions, respectively. The experimental results have successfully validated the effectiveness of the proposed approach. The singularity-free property and stability of the developed control system is demonstrated by accomplishing a large angle maneuver under undesirable initial conditions.

5. CONCLUSION

Utilizing the quaternion attitude representation, the UDE-based attitude and position controllers have been developed for a quadrotor to achieve the robust global control while dealing with model uncertainties and external disturbances. Flight experiments were performed to demonstrate the capabilities of the developed controllers for recovering from undesirable large initial angles. More experimental cases, which consider the effects of the external disturbances, such as wind, and the model uncertainties, such as mass and inertia variations and the performance comparison with available control methods will be investigated in the journal version of this article.

REFERENCES

Chen, F., Jiang, R., Zhang, K., Jiang, B., and Tao, G. (2016). Robust backstepping sliding-mode control and observer-based fault estimation for a quadrotor UAV. *IEEE Transactions on Industrial Electronics*, 63(8), 5044–5056.

Cutler, M. and How, J.P. (2015). Analysis and control of a variable-pitch quadrotor for agile flight. *ASME Journal of Dynamic Systems, Measurement, and Control*, 137(10), 101002.

Dai, J., Ren, B., and Zhong, Q.C. (2018). Uncertainty and disturbance estimator-based backstepping control for nonlinear systems with mismatched uncertainties and disturbances. *ASME Journal of Dynamic Systems, Measurement, and Control*, 140(12), 121005.

D.H.S. Maithripala and Jordan M. Berg (2015). An intrinsic PID controller for mechanical systems on Lie groups. *Automatica*, 54, 189–200.

Faessler, M., Fontana, F., Forster, C., and Scaramuzza, D. (2015). Automatic re-initialization and failure recovery for aggressive flight with a monocular vision-based quadrotor. In *Proceedings of the IEEE International Conference on Robotics and Automation*, 1722–1729. Seattle, WA, USA.

Goodarzi, F.A., Lee, D., and Lee, T. (2015). Geometric adaptive tracking control of a quadrotor UAV on SE (3) for agile maneuvers. *ASME Journal of Dynamic Systems, Measurement, and Control*, 137(9), 20–32.

Lee, T. (2013). Robust adaptive attitude tracking on SO(3) with an application to a quadrotor UAV. *IEEE Transactions on Control Systems Technology*, 21(5), 1924–1930.

Liu, H., Wang, X., and Zhong, Y. (2015). Quaternion-based robust attitude control for uncertain robotic quadrotors. *IEEE Transactions on Industrial Informatics*, 11(2), 406–415.

Lu, Q., Ren, B., and Parameswaran, S. (2018). Shipboard landing control enabled by an uncertainty and disturbance estimator. *AIAA Journal of Guidance, Control, and Dynamics*, 41(7), 1502–1520.

Lu, Q., Ren, B., Parameswaran, S., and Zhong, Q.C. (2017). Uncertainty and disturbance estimator-based robust trajectory tracking control for a quadrotor in a global positioning system-denied environment. *ASME Journal of Dynamic Systems, Measurement, and Control*, 140(3), 031001.

Mahony, R., Hamel, T., and Pflimlin, J. (2008). Nonlinear complementary filters on the special orthogonal group. *IEEE Transactions on Automatic Control*, 53(5), 1203–1218.

Markley, F.L. (2002). Fast quaternion attitude estimation from two vector measurements. *AIAA Journal of Guidance, Control, and Dynamics*, 25(2), 411–414.

Moreno-Valenzuela, J., Perez-Alcocer, R., Guerrero-Medina, M., and Dzul, A. (2018). Nonlinear PID-type controller for quadrotor trajectory tracking. *IEEE/ASMETransactions on Mechatronics*, 23(5), 2436–2447.

Naldi, R., Furci, M., Sanfelice, R.G., and Marconi, L. (2017). Robust global trajectory tracking for underactuated VTOL aerial vehicles using inner-outer loop control paradigms. *IEEE Transactions on Automatic Control*, 62(1), 97–112.

Ren, B., Zhong, Q.C., and Dai, J. (2017). Asymptotic reference tracking and disturbance rejection of UDE-based robust control. *IEEE Transactions on Industrial Electronics*, 64(4), 3166–3176.

Sanz, R., Garcia, P., Zhong, Q.C., and Albertos, P. (2016). Robust control of quadrotors based on an uncertainty and disturbance estimator. *ASME Journal of Dynamic Systems, Measurement, and Control*, 138(7), 071006.

Shi, X., Zhang, Y., and Zhou, D. (2017). Almost-global finite-time trajectory tracking control for quadrotors in the exponential coordinates. *IEEE Transactions on Aerospace and Electronic Systems*, 53(1), 91–100.

Tayebi, A. (2008). Unit quaternion-based output feedback for the attitude tracking problem. *IEEE Transactions on Automatic Control*, 53(6), 1516–1520.

Tayebi, A. and McGilvray, S. (2006). Attitude stabilization of a VTOL quadrotor aircraft. *IEEE Transactions on Control Systems Technology*, 14(3), 562–571.

Yang, H., Cheng, L., Xia, Y., and Yuan, Y. (2018). Active disturbance rejection attitude control for a dual closed-loop quadrotor under gust wind. *IEEE Transactions on Control Systems Technology*, 26(4), 1400–1405.

Zhao, B., Xian, B., Zhang, Y., and Zhang, X. (2015). Nonlinear robust adaptive tracking control of a quadrotor UAV via immersion and invariance methodology. *IEEE Transactions on Industrial Electronics*, 62(5), 2891–2902.

Zhong, Q.C. and Rees, D. (2004). Control of uncertain LTI systems based on an uncertainty and disturbance estimator. *ASME Journal of Dynamic Systems, Measurement, and Control*, 126(4), 905–910.